

# TabKAN: Advancing Tabular Data Analysis using Kolmogorov-Arnold Network

Ali Eslamian<sup>1</sup>, Alireza Afzal Aghaei<sup>2</sup>, Qiang Cheng<sup>1,3</sup>

<sup>1</sup>Department of Computer Science, University of Kentucky, 329 Rose Street, Lexington, KY 40506, USA.

<sup>2</sup>Independent Researcher.

<sup>3</sup>Institute for Biomedical Informatics, University of Kentucky, 800 Rose Street, Lexington, KY 40506, USA.

## Abstract

Tabular data analysis presents unique challenges due to its heterogeneous feature types, missing values, and complex interactions. While traditional machine learning methods, such as gradient boosting, often outperform deep learning approaches, recent advancements in neural architectures offer promising alternatives. This paper introduces TabKAN, a novel framework that advances tabular data modeling using Kolmogorov-Arnold Networks (KANs). Unlike conventional deep learning models, KANs leverage learnable activation functions on edges, enhancing both interpretability and training efficiency. Our contributions include: (1) the introduction of modular KAN-based architectures tailored for tabular data analysis, (2) the development of a transfer learning framework for KAN models, enabling effective knowledge transfer between domains, (3) the development of model-specific interpretability for tabular data learning, reducing reliance on post hoc and model-agnostic analysis, and (4) comprehensive evaluation of vanilla supervised learning across binary and multi-class classification tasks. Through extensive benchmarking on diverse public datasets, TabKAN demonstrates superior performance in supervised learning while significantly outperforming classical and Transformer-based models in transfer learning scenarios. Our findings highlight the advantage of KAN-based architectures in efficiently transferring knowledge across domains, bridging the gap between traditional machine learning and deep learning for structured data.

## 1 Introduction

Tabular data is a fundamental form of structured data prevalent across diverse domains, ranging from healthcare and finance to e-commerce and scientific research. Analyzing such data efficiently and accurately is critical for deriving actionable insights and advancing decision-making processes. Despite the significant progress achieved in deep learning, particularly in image and text processing, tabular data analysis remains a challenging domain due to its unique characteristics, such as heterogeneous feature types, missing values, and complex feature interactions. While traditional machine learning methods, such as tree-based models, have frequently demonstrated superior performance compared to deep learning approaches in this domain, the development of novel architectures specifically designed for tabular data remains crucial.

In recent years, the potential of neural networks for tabular data modeling has gained significant attention. Among these, Kolmogorov-Arnold Networks have emerged as a promising alternative to traditional Multi-Layer Perceptrons, addressing key challenges such as interpretability, training efficiency and robustness. Unlike MLPs, which rely on fixed activation functions at nodes, KANs feature learnable activation functions on edges, enabling more flexible and efficient modeling of complex feature interactions. Inspired by the Kolmogorov-Arnold representation theorem, which expresses any multivariate continuous function as a composition of univariate functions and a summation operator, KANs provide a structured framework for tabular data analysis.

This paper introduces TabKAN, an encompassing framework for numerical and categorical feature encoding through a KAN-based Module specifically designed for tabular data modeling using various KAN-based architectures, including spl-KAN [1], ChebyshevKAN [2], RKAN [3], Fourier KAN [4], fKAN [5] and Fast-KAN [6]. Due to the inherent diversity and complexity of patterns present in tabular datasets, TabKAN leverages multiple KAN variants, enabling flexible adaptation and enhanced representation capabilities tailored to different data characteristics. The primary novelties of this study are:

- The introduction of modular KAN-based architectures tailored for tabular data analysis
- The development of a transfer learning framework for KAN models, enabling effective knowledge transfer between domains
- The creation of model-specific interpretability methods for tabular data learning, reducing reliance on post hoc and model-agnostic analysis
- A comprehensive evaluation of vanilla supervised learning across binary and multi-class classification tasks

TabKAN demonstrates stable and significantly improved performance in supervised learning and transfer learning tasks outperforming baseline models in binary and multi-class classification across diverse public datasets. By applying KAN principles, TabKAN unifies traditional machine learning and deep learning, providing a robust, interpretable, and efficient solution for tabular data modeling.

## 2 Related Work

Existing methods for tabular learning face multiple obstacles, such as mismatched feature sets between training and testing, limited or missing labels, and the potential emergence of new features over time [7]. It can be categorized as:

**Classic Machine Learning Models.** Early techniques rely on parametric or non-parametric strategies like K-Nearest Neighbors (KNN), Gradient Boosting, Decision Trees, and Logistic Regression [8]. Popular models include Logistic Regression (LR), XGBoost [9, 10], and MLP. A notable extension is the self-normalizing neural network (SNN) [11], which employs scaled exponential linear units (SELU) to maintain neuron activations at zero mean and unit variance. While SNNs are straightforward and effective, they can struggle with complex, high-dimensional data, prompting the development of more advanced neural architectures.

**Deep Learning-Based Supervised Models.** Building on Transformer architectures, methods such as AutoInt [12] use self-attention to learn feature importance, while TransTab [13] extends Transformers to handle partially overlapping columns across multiple tables, enabling tasks like transfer learning, incremental feature learning, and zero-shot inference. Similarly, TabTransformer [14] applies self-attention to enhance feature embeddings, achieving robust performance even with missing data. SAINT [15] introduces a hybrid attention scheme at both row and column levels, pairing it with inter-sample attention and contrastive pre-training, and surpasses gradient boosting models including XGBoost [9], CatBoost [16], and LightGBM [17] on various benchmarks. Other innovations include TabRet [18], which implements a retokenization step for previously unseen columns, and XTab [19], which enables cross-table pretraining in a federated learning setup, managing heterogeneous column types and numbers. TabCBM [20] provides concept-based explanations that allow human oversight, thereby striking a balance between strong predictive accuracy and transparent, understandable reasoning. TabPFN [21] is a pretrained Transformer-based model that performs zero-shot classification on tabular data by leveraging meta-learning, eliminating the need for task-specific training. TabMap [22] transforms tabular data into 2D topographic maps that spatially encode feature relationships and preserve values as pixel intensities, allowing convolutional neural networks to efficiently extract association patterns and outperform other deep learning-based supervised models. TabSAL [23] employs lightweight language models to generate privacy-free synthetic tabular data when raw data cannot be shared due to privacy risks. TabMixer [24] is an enhanced MLP-mixer-based architecture that captures both sample-wise and feature-wise interactions using a self-attention mechanism.

## 3 Background

### 3.1 Data Preprocessing

In order to handle missing values and class imbalance we used the preprocessing method in [24]. Let the input variable space as  $Data \in \{\mathbb{R} \cup \mathbb{C} \cup \mathbb{B} \cup \emptyset\}$ , where  $\mathbb{R}$ ,  $\mathbb{C}$ , and  $\mathbb{B}$  represent the domains of numerical, categorical, and binary data, respectively. After preprocessing block, we have  $\{\mathcal{X}, \mathcal{Y}\}$  denote a feature-target pair, where  $x$  represents numerical features, and  $y$  is integer number for classification tasks.  $\{\mathcal{Y}\}$  can have dimension of one for binary classification or  $M$  for multi-class classification.

In most tables, the data consists of both continuous numerical and categorical variables. We preprocess the categorical features by transforming them into one-hot vectors. After the preprocessing step, the data is represented as  $n \times m$  matrix, where all entries are numerical values.

### 3.2 Kolmogorov–Arnold Networks (KANs)

A general KAN network is a composition of  $L$  layers. Given  $\mathbf{x}_0 \in \mathbb{R}^{n_0}$ , the output is

$$\text{KAN}(\mathbf{x}_0) = (\Phi_{L-1} \circ \dots \circ \Phi_0) \mathbf{x}_0$$

For scalar outputs (i.e.,  $n_L = 1$ ), we denote

$$f(\mathbf{x}) = \text{KAN}(\mathbf{x})$$

and it can be expanded analogously using a nested summation form. The original Kolmogorov–Arnold representation [25] corresponds to a 2-layer KAN of shape  $[n, 2n+1, 1]$ ; nonlinearities sit on the edges, while each node simply sums its inputs. A natural way to approach the underlying approximation problem is by selecting appropriate univariate functions  $\phi_{q,p}$  and  $\Phi_q$ . In this setup, the middle layer has width  $2n+1$ . However, a two-layer spline-based network often lacks sufficient expressivity for complex tasks. Consequently, we generalize the KAN design by making it both deeper and wider.

This construction mirrors that of Multi-Layer Perceptrons (MLPs), where a single layer, an affine transformation followed by a nonlinearity, is stacked to increase model capacity. Similarly, we define a KAN layer and compose multiple such layers to build a deeper, more expressive model.

Let the network’s shape be an integer array

$$[n_0, n_1, \dots, n_L]$$

where  $n_\ell$  denotes the number of nodes in the  $\ell$ -th layer. Denote the activation of the  $i$ -th neuron in the  $\ell$ -th layer by  $x_{\ell,i}$ . Between layer  $\ell$  and layer  $\ell+1$ , there are  $n_\ell \times n_{\ell+1}$  univariate functions  $\phi_{\ell,j,i}$ . For the connection from neuron  $(\ell, i)$  to  $(\ell+1, j)$ , the input is  $x_{\ell,i}$  and the output (post-activation) is

$$\tilde{x}_{\ell,j,i} = \phi_{\ell,j,i}(x_{\ell,i})$$

Each neuron  $(\ell+1, j)$  sums all post-activations from its incoming edges:

$$x_{\ell+1,j} = \sum_{i=1}^{n_\ell} \phi_{\ell,j,i}(x_{\ell,i})$$

In matrix form, layer  $\ell$  can be expressed as

$$\mathbf{x}_{\ell+1} = \begin{pmatrix} \phi_{\ell,1,1}(\cdot) & \cdots & \phi_{\ell,1,n_\ell}(\cdot) \\ \vdots & \ddots & \vdots \\ \phi_{\ell,n_{\ell+1},1}(\cdot) & \cdots & \phi_{\ell,n_{\ell+1},n_\ell}(\cdot) \end{pmatrix} \mathbf{x}_\ell$$

where  $\Phi_\ell$  is the “function matrix” for the  $\ell$ -th KAN layer. Stacking these KAN layers yields a deep KAN with greater flexibility and expressive power than the simple two-layer variant.

### 3.3 General KAN Layer

To define a KAN layer with  $n_{\text{in}}$ -dimensional inputs and  $n_{\text{out}}$ -dimensional outputs, consider a matrix of one-dimensional functions:

$$\Phi = \{\phi_{q,p}\}, \quad p = 1, \dots, n_{\text{in}}, \quad q = 1, \dots, n_{\text{out}}$$

where each  $\phi_{q,p}$  has trainable parameters. In the original Kolmogorov–Arnold theorem, the “inner” functions form a KAN layer with  $n_{\text{in}} = n$  and  $n_{\text{out}} = 2n + 1$ , while the “outer” functions form another KAN layer with  $n_{\text{in}} = 2n + 1$  and  $n_{\text{out}} = 1$ . Since these operations are all differentiable, we train KANs through standard backpropagation.

### 3.4 Chebyshev Kolmogorov-Arnold Network Layer (ChebyKAN)

The ChebyKANLayer [2] employs Chebyshev polynomials of the first kind,  $\{T_k(x)\}_{k=0}^d$ , to approximate nonlinear functions with fewer parameters than traditional MLPs. First, the input  $\mathbf{x} \in \mathbb{R}^n$  is normalized to  $[-1, 1]$  via the hyperbolic tangent function:

$$\tilde{\mathbf{x}} = \tanh(\mathbf{x})$$

The Chebyshev polynomials are then computed up to degree  $d$  using the recursive definition

$$\begin{aligned} T_0(x) &= 1, \\ T_1(x) &= x, \\ T_k(x) &= 2xT_{k-1}(x) - T_{k-2}(x), \quad \text{for } k \geq 2. \end{aligned}$$

yielding a polynomial tensor  $\mathbf{T}$ .

Let  $\Theta \in \mathbb{R}^{n \times m \times (d+1)}$  be the trainable coefficient tensor for  $n$  input features,  $m$  outputs, and polynomial degree  $d + 1$ . The layer output is computed via Einstein summation:

$$y_{bo} = \sum_{i=1}^n \sum_{k=0}^d T_{bik} \Theta_{iok} \quad (1)$$

where  $b$  indexes the batch. By optimizing  $\Theta$  during training, ChebyKAN learns a highly expressive mapping with exceptional accuracy, capitalizing on the orthogonality and rapid convergence of Chebyshev polynomials.

### 3.5 Fast Kolmogorov-Arnold Network (Fast KAN)

FastKAN [6] is a reengineered variant of KAN designed to significantly enhance computational efficiency by replacing the original 3<sup>rd</sup>-order B-spline basis with Gaussian radial basis functions (RBFs). In this framework, Gaussian RBFs serve as the primary nonlinear transformation, effectively approximating the B-spline operations used in traditional KAN. In addition,

it applies layer normalization [26] to keep inputs from drifting outside the effective range of these RBFs. Together, these adjustments simplify the overall design of FastKAN while preserving its accuracy. The output of an RBF network is a weighted linear combination of these radial basis functions. Mathematically, an RBF network with  $N$  centers can be expressed as:

$$f(x) = \sum_{i=1}^N w_i \phi(\|\mathbf{x} - \mathbf{c}_i\|)$$

where  $w_i$  are the learnable parameters or coefficients, and  $\phi$  is the radial basis function, which depends on the distance between the input  $x$  and a center  $c_i$  represented as:

$$\phi(r) = \exp\left(-\frac{r^2}{2h^2}\right)$$

While standard KAN consists of sums of univariate transformations to approximate multivariate functions, Fast KAN generalizes this principle in a deeper feedforward architecture. For an input vector  $\mathbf{x} \in \mathbb{R}^d$ , the output is computed as

$$\mathbf{y} = f_L \circ f_{L-1} \circ \cdots \circ f_1(\mathbf{x})$$

We optimize the number of layers  $L$  and the width vector  $\mathbf{w} = (w_1, \dots, w_L)$  as hyperparameters to adapt the Fast KAN architecture to different datasets. This includes both the number of layers and the neurons per layer. Additionally, the parameters of the RBF activation functions (e.g., centers and bandwidths) can be tuned or learned. To efficiently explore architectural configurations, we employ the automated hyperparameter optimization framework Optuna [27], selecting the settings that maximize validation performance (F1 Score).

### 3.6 Padé Rational Kolmogorov-Arnold Network (PadéRKAN)

The Padé Rational Kolmogorov-Arnold Network (PadéRKAN) [3] augments the Kolmogorov-Arnold framework by adopting the Padé approximation, which expresses a function as the ratio of two polynomials:

$$R(x) = \frac{P_q(x)}{Q_k(x)} = \frac{\sum_{i=0}^q a_i x^i}{\sum_{j=0}^k b_j x^j}$$

In each PadéRKAN layer, this rational form serves as the activation function, enabling the model to capture asymptotic behavior and abrupt transitions more accurately. Specifically, for an input  $\mathbf{x} \in \mathbb{R}^d$ , the layer outputs

$$\mathbf{y} = \frac{\sum_{i=0}^q \theta_i P_i(\mathbf{x})}{\sum_{j=0}^k \theta_j Q_j(\mathbf{x})}$$

where  $\theta_i$  and  $\theta_j$  are learnable parameters for the numerator and denominator polynomials, respectively.

By tuning the network depth, layer widths, and polynomial degrees  $(q, k)$  with Optuna, PadéRKAN adapts to various datasets and task complexities, while the L-BFGS optimizer minimizes the cross-entropy loss. Due to its rational formulation, PadéRKAN is capable of

approximating functions characterized by sharp transitions and asymptotic behaviors, thereby providing enhanced modeling flexibility relative to purely polynomial-based KAN variants.

### 3.7 Fourier Kolmogorov-Arnold Network (Fourier KAN)

Fourier KAN [28] leverages a Fourier series expansion to capture both low- and high-frequency components in tabular or structured data. Given an input vector  $\mathbf{x} \in \mathbb{R}^d$ , the transformation function  $\phi_F(\mathbf{x})$  introduces sine and cosine terms up to a grid size  $g$ , thus enabling the network to approximate highly complex or oscillatory functions. Formally,

$$\phi_F(\mathbf{x}) = \sum_{i=1}^d \sum_{k=1}^g (a_{ik} \cos(k x_i) + b_{ik} \sin(k x_i))$$

where  $a_{ik}$  and  $b_{ik}$  are trainable coefficients. The hyperparameter  $g$  controls the number of frequency components and balances representational power against computational cost.

A Fourier KAN layer applies this frequency-based feature mapping to each input dimension and then combines the resulting terms via learnable parameters. For example, an output neuron  $y$  is computed as:

$$y = \sum_{i=1}^d \sum_{k=1}^g (W_{ik}^{(c)} \cos(k x_i) + W_{ik}^{(s)} \sin(k x_i)) + b \quad (2)$$

where  $W_{ik}^{(c)}$  and  $W_{ik}^{(s)}$  are learnable weights for the cosine and sine terms, respectively, and  $b$  is a bias. By capitalizing on the orthogonality of trigonometric functions, Fourier KAN often converges faster than traditional MLPs and polynomial-based KANs while reducing overfitting. In practice, tuning the grid size  $g$  is critical to accommodate the desired frequency range and optimize performance on diverse datasets.

### 3.8 Fractional Kolmogorov-Arnold Network (fKAN)

The Fractional Kolmogorov-Arnold Network (fKAN) [29] incorporates fractional-order Jacobi polynomials into the Kolmogorov-Arnold framework to enhance expressiveness and adaptability. Each layer of fKAN uses a Fractional Jacobi Neural Block (fJNB), which introduces a trainable fractional parameter  $\nu$  to adjust the polynomial basis dynamically. For an input  $\mathbf{x} \in \mathbb{R}^d$ , the fractional Jacobi polynomial  $J_n^{(\alpha, \beta, \nu)}(x)$  is given by:

$$J_n^{(\alpha, \beta)}(x^\nu) = \frac{(\alpha + 1)_n}{n!} \sum_{k=0}^n \binom{n}{k} \frac{(\beta + 1)_{n-k}}{(\alpha + \beta + 1)_{n-k}} \left(\frac{x^\nu - 1}{2}\right)^k \left(\frac{x^\nu + 1}{2}\right)^{n-k}$$

where  $(\alpha, \beta) > -1$  determine the shape of the polynomial, and  $B(\cdot, \cdot)$  denotes the Beta function.

Within fKAN, each layer applies a linear transformation followed by a fractional Jacobi activation, enabling the model to capture subtle data patterns. Hyperparameters such as network depth, layer widths, and the fractional order  $\nu$  are tuned with Optuna, and training is performed using the L-BFGS optimizer to minimize cross-entropy loss. By allowing the

polynomial order to be learned, fKAN can adapt its functional complexity to a wide range of datasets, often yielding improved generalization as evidenced by metrics like F1 score and ROC-AUC.

### 3.9 Rational Kolmogorov-Arnold Network (RKAN)

The Jacobi Rational Kolmogorov-Arnold Network (RKAN) [30] integrates Jacobi polynomials  $J_n^{(\alpha, \beta)}(x)$  and a rational mapping  $\phi(x, L) = \frac{x}{\sqrt{x^2+L^2}}$  to enhance nonlinear function approximation beyond the conventional  $[-1, 1]$  domain. For an input  $\mathbf{x} \in \mathbb{R}^d$ , the layer output is formulated as:

$$\mathbf{y} = \sum_{n=0}^N \theta_n J_n^{(\alpha, \beta)}(\phi(\mathbf{x}, L))$$

where  $\theta_n$  and  $L$  are trainable coefficients and  $\alpha, \beta > -1$  specify the polynomial's orthogonality weight function  $\omega(x) = (1-x)^\alpha(1+x)^\beta$ . The mapping  $\phi(x, L)$  extends the polynomials to the infinite interval, making it needless for data scaling.

RKAN leverages Optuna to adaptively choose the network depth, layer widths, and polynomial orders, and employs the L-BFGS optimizer to minimize cross-entropy loss. By combining rational mapping with Jacobi polynomials, RKAN effectively models asymptotic behavior and achieves robust performance across various datasets, as evidenced by metrics such as F1 score and ROC-AUC.

## 4 Experiments and Results

We thoroughly evaluate our model using ten publicly available datasets covering supervised and transfer learning scenarios. Although we use several performance metrics—AUC, F1 score, precision, and recall—we report only AUC due to its effectiveness in summarizing classification performance and space constraints. To assess robustness, we benchmark our model against state-of-the-art methods with varying data and feature usage, using average ranking as the primary comparison metric, following the protocol of [13], which offers a holistic view of relative performance across datasets.

### 4.1 Datasets

We employ a variety of datasets to evaluate our models, covering a broad spectrum of application areas:

- **Financial Decision-Making:** Credit-g (CG) and Credit-Approval (CA) datasets
- **Retail:** Dresses-sale (DS) dataset, capturing detailed sales transactions
- **Demographic Analysis:** Adult (AD) and 1995-income (IO) datasets, containing income and census-related variables
- **Specialized Industries:**
  - Cylinder bands (CB) dataset for manufacturing
  - Blastchar (BL) dataset for materials science
  - Insurance company (IC) dataset offering insights into the insurance domain

Collectively, these benchmark datasets span diverse fields and data structures, enabling a thorough assessment of our approach. Additional details for each dataset appear in Table 1.

**Table 1:** Dataset details including abbreviation, number of classes, number of data points, and number of features.

Dataset Name	Abbreviation	# Class	# Data	# Features
Credit-g	CG	2	1,000	20
Credit-Approval	CA	2	690	15
Dataset-Sales	DS	2	500	12
Adult	AD	2	48,842	14
Cylinder-Bands	CB	2	540	35
Blastchar	BL	2	7,043	35
Insurance-Co	IO	2	5,822	85
1995-Income	IC	2	32,561	14
ImageSegmentation	SG	7	2,310	20
ForestCovertype	FO	7	581,012	55

We choose the configuration that yields the highest validation performance and then train the model on each dataset using ten distinct random seeds to mitigate the impact of training variability. This procedure aligns with the comparative approach used in TabMixer [24]. All experiments run on an AMD Ryzen Threadripper PRO 5965WX 24-core CPU with 62 GB of RAM and an NVIDIA RTX A4500 GPU featuring 20 GB of memory.

## 4.2 Baseline Models for Comparison

We benchmark our proposed model against both classic and cutting-edge techniques, including **Logistic Regression (LR)**, **XGBoost** [9], **MLP**, **SNN** [11], **TabNet** [31], **DCN** [32], **AutoInt** [12], **TabTransformer** [14], **FT-Transformer** [33], **VIME** [34], **SCARF** [35], **CatBoost** [16], **SAINT** [15], and **TransTab** [13]. These baselines span a range of approaches for tabular data, from traditional machine learning to the latest deep learning methods.

To ensure a fair comparison, we apply the same preprocessing and evaluation workflow across all models. After preprocessing, each dataset is divided into training, validation, and test sets with a 70/10/20 split.

## 4.3 Supervised Learning

Table 2 presents results from evaluating classical baselines (Logistic Regression, XGBoost, MLP, SNN), specialized tabular models (TabNet, DCN, AutoInt, TabTrans, FT-Trans, VIME, SCARF, TransTab), and a range of KAN variants (ChebyshevKAN, JacobiKAN, PadeKAN, Fourier KAN, fKAN, fast-KAN) alongside the original KAN architecture. Each approach is optimized individually, with hyperparameters tuned to account for differences in model structure and dataset characteristics. The results show Chebyshev KAN emerges as the top performer, suggesting that its Chebyshev polynomial basis effectively captures intricate

decision boundaries while maintaining stability. However, certain KAN variants, such as wav-KAN [36], did not show strong performance on any dataset, while others, like fc-KAN [37], feature a heavier architecture that limits practical applicability. This highlights the inherent difficulty of designing a single architecture that performs uniformly well across diverse data distributions, leading us to exclude them from our final results.

The KAN-based methods consistently outperform conventional baselines and, in many cases, are comparable to or surpass transformer-based architectures. This highlights the expressive power of the Kolmogorov-Arnold framework. Our experiments underscore the importance of careful model selection and tuning of architectural and layer-specific parameters. Moreover, the broad success of KAN variants demonstrates how leveraging polynomial, rational, or Fourier expansions can significantly improve learning on tabular data.

**Table 2:** Evaluation of Different Models for Supervised Learning

Methods	CG	CA	DS	AD	CB	BL	IO	IC	Rank (Std) ↓	Average ↑
Logistic Regression	0.720	0.836	0.557	0.851	0.748	0.801	0.769	0.860	17 (2.45)	0.768
XGBoost	0.726	0.895	0.587	0.912	<b>0.892</b>	0.821	0.758	0.925	9.06 (6.67)	0.814
MLP	0.643	0.832	0.568	0.904	0.613	0.832	0.779	0.893	15.3 (3.13)	0.758
SNN	0.641	0.880	0.540	0.902	0.621	0.834	0.794	0.892	13.6 (4.73)	0.763
TabNet	0.585	0.800	0.478	0.904	0.680	0.819	0.742	0.896	17.1 (3.49)	0.738
DCN	0.739	0.870	0.674	<u>0.913</u>	0.848	0.840	0.768	0.915	7.69 (4.12)	0.821
AutoInt	0.744	0.866	0.672	<u>0.913</u>	0.808	<u>0.844</u>	0.762	0.916	7.94 (4.63)	0.816
TabTrans	0.718	0.860	0.648	<b>0.914</b>	0.855	<u>0.820</u>	0.794	0.882	11.1 (5.85)	0.811
FT-Trans	0.739	0.859	0.657	<u>0.913</u>	<u>0.862</u>	0.841	0.793	0.915	8.19 (4.46)	0.822
VIME	0.735	0.852	0.485	0.912	0.769	0.837	0.786	0.908	11.8 (4.58)	0.786
SCARF	0.733	0.861	0.663	0.911	0.719	0.833	0.758	0.919	11 (4.56)	0.800
TransTab	0.768	0.881	0.643	0.907	0.851	0.845	0.822	0.919	<u>6.88 (3.43)</u>	0.830
TabMixer	0.660	<b>0.907</b>	0.659	0.900	0.829	0.821	0.974	<b>0.969</b>	7.94 (6.54)	0.840
<b>KAN</b>	0.806	0.870	0.616	0.907	0.739	0.844	0.956	0.902	8.69 (4.11)	0.83
<b>ChebyshevKAN</b>	0.823	0.883	0.670	0.905	<u>0.862</u>	<b>0.859</b>	0.951	0.905	<b>5.88 (3.47)</b>	<b>0.857</b>
<b>JacobiKAN</b>	<b>0.854</b>	0.860	0.685	0.888	0.611	0.814	0.957	0.885	11.5 (7.69)	0.819
<b>PadeKAN</b>	0.826	0.855	0.670	0.868	0.778	0.808	0.952	0.856	12.4 (6.52)	0.827
<b>Fourier KAN</b>	0.771	0.870	0.650	0.906	0.820	0.649	0.879	<u>0.935</u>	9.31 (5.08)	0.810
<b>fKAN</b>	<u>0.848</u>	0.870	<b>0.691</b>	0.892	0.692	0.811	0.954	0.890	10.2 (6.64)	0.831
<b>fast-KAN</b>	<b>0.854</b>	<u>0.897</u>	<u>0.688</u>	0.892	0.767	0.837	<b>0.960</b>	0.887	7.44 (6.55)	<u>0.848</u>

Supervised learning requires ample labeled data; however, recent studies improve analysis using hybrid domain-specific methods [38], multimodal approaches that combine language models with tabular inputs [39], or integrations of vision and tabular data for medical prediction tasks [40].

#### 4.4 Transfer Learning

Transfer learning enables machine learning models to leverage knowledge acquired from a source task to improve performance on a related target task through fine-tuning. While this paradigm has proven effective in domains like computer vision and natural language processing, where shared structures simplify knowledge transfer, its application to tabular data presents unique challenges. Feature heterogeneity, dataset-specific distributions, and the absence of universal structural patterns often lead to encoder overspecialization during

conventional supervised pretraining. In this scenario, models trained on classification objective develop representations overly tailored to dominant patterns in the source data, which can limit their adaptability to target tasks with divergent feature spaces, class imbalances, or objectives.

To systematically evaluate transfer learning in tabular settings, we adopt the methodology of [13], partitioning each dataset into two subsets (Set1 and Set2) with a controlled 50% feature overlap. This design introduces a domain shift by treating overlapping features as shared knowledge and non-overlapping features as distinct statistical domains. The partial overlap allows assessment of the model’s ability to generalize shared representations while adapting to novel features.

This process involves two primary stages: pretraining and fine-tuning. During pretraining, the model is trained on Set1 using supervised learning to acquire initial feature representations. Upon convergence, the learned patterns are preserved by freezing all layers except the final main layer (and bias layer, if applicable). Subsequently, the model undergoes fine-tuning on Set2, where only the unfrozen layers are updated. This selective updating allows the model to adapt to the target data distribution of Set2 while retaining the knowledge acquired from Set1.

To validate robustness, we evaluate the model on the test split of Set2, measuring its capacity to generalize under domain shifts. Additionally, we reverse the roles of Set1 and Set2 in a cross-validation framework, ensuring comprehensive evaluation of bidirectional knowledge transfer. This approach enables TabKAN to balance representation stability (via frozen layers) and adaptability (via targeted fine-tuning), addressing the challenges of feature heterogeneity and encoder overspecialization in tabular data.

The results shows that Fourier KAN outperforms all other architectures, suggesting that its kernel approximation via Fourier series provides a strong inductive bias for knowledge transfer. The smooth, periodic basis functions in Fourier expansions help capture recurring patterns in the data, thereby enabling more effective generalization to new domains.

**Table 3:** Evaluation of Models for Transfer Learning

Methods	CG		CA		DS		AD		CB		BL		IO		IC		Rank(Std) ↓	Average ↑
	set1	set2																
Logistic Regression	0.69	0.69	0.81	0.82	0.47	0.56	0.81	0.81	0.68	0.78	0.77	0.82	0.71	0.81	0.81	0.84	14.5 (2.82)	0.736
XGBoost	0.72	0.71	0.85	0.87	0.46	0.63	0.88	0.89	0.80	0.81	0.76	0.82	0.65	0.74	0.92	0.91	9.53 (5.38)	0.776
MLP	0.67	0.70	0.82	0.86	0.53	0.67	0.89	0.90	0.73	0.82	0.79	0.83	0.70	0.78	0.90	0.90	9.84 (4.23)	0.775
SNN	0.66	0.63	0.85	0.83	0.54	0.42	0.87	0.88	0.57	0.54	0.77	0.82	0.69	0.78	0.87	0.88	14.5 (3.90)	0.727
TabNet	0.60	0.47	0.66	0.68	0.54	0.53	0.87	0.88	0.58	0.62	0.75	0.83	0.62	0.71	0.88	0.89	15.9 (4.09)	0.692
DCN	0.69	0.70	0.83	0.85	0.51	0.58	0.88	0.74	0.79	0.78	0.79	0.76	0.70	0.71	0.91	0.90	11.4 (4.51)	0.758
AutoInt	0.70	0.70	0.82	0.86	0.49	0.55	0.88	0.74	0.77	0.79	0.79	0.76	0.71	0.72	0.91	0.90	11.6 (4.39)	0.754
TabTrans	0.72	0.72	0.84	0.86	0.54	0.57	0.88	<b>0.90</b>	0.73	0.79	0.78	0.81	0.67	0.71	0.88	0.88	11.5 (3.57)	0.764
FT-Trans	0.72	0.71	0.83	0.85	0.53	0.64	0.89	0.90	0.76	0.79	0.78	0.84	0.68	0.78	0.91	<b>0.91</b>	8.84 (3.82)	0.781
VIME	0.59	0.70	0.79	0.76	0.45	0.53	0.88	<b>0.90</b>	0.65	0.81	0.58	0.83	0.67	0.70	0.90	0.90	14.5 (5.37)	0.718
SCARF	0.69	0.72	0.82	0.85	0.55	0.64	0.88	<b>0.89</b>	0.77	0.73	0.78	0.83	0.71	0.75	0.90	0.89	10.1 (2.87)	0.778
TransTab	0.74	0.76	0.87	<b>0.89</b>	0.55	0.66	0.88	<b>0.90</b>	<b>0.80</b>	0.80	0.79	0.84	0.73	0.82	0.91	<b>0.91</b>	5.56 (2.17)	0.803
TabMixer	<b>0.86</b>	0.84	0.87	0.88	0.64	<b>0.71</b>	<b>0.90</b>	<b>0.90</b>	<b>0.94</b>	0.77	<b>0.93</b>	<b>0.92</b>	<b>0.95</b>	<b>0.95</b>	<b>0.94</b>	<b>0.95</b>	<b>1.91 (1.14)</b>	<b>0.883</b>
<b>KAN</b>	0.80	0.81	0.88	0.86	0.50	0.50	0.56	0.64	0.73	0.74	0.84	0.85	<b>0.95</b>	<b>0.95</b>	0.90	0.90	9.19 (6.18)	0.774
ChebyshevKAN	0.79	0.76	<b>0.89</b>	<b>0.89</b>	0.60	0.60	0.84	0.88	0.77	0.50	0.65	<b>0.86</b>	<b>0.91</b>	0.89	0.82	0.82	8.38 (5.71)	0.796
JacobiKAN	<b>0.85</b>	<b>0.86</b>	0.85	0.86	0.66	0.68	0.86	0.88	0.61	0.61	0.82	<b>0.95</b>	<b>0.95</b>	0.88	0.88	8.28 (5.88)	0.814	
PadeKAN	0.76	0.77	0.87	0.80	0.50	0.62	0.86	0.50	0.64	0.64	0.66	0.88	0.76	0.63	0.50	13.7 (5.51)	0.691	
Fourier KAN	0.83	0.82	<b>0.89</b>	<b>0.88</b>	<b>0.67</b>	<b>0.68</b>	<b>0.90</b>	<b>0.90</b>	<b>0.86</b>	<b>0.86</b>	<b>0.85</b>	<b>0.95</b>	<b>0.95</b>	<b>0.95</b>	0.90	2.72 (1.56)	<b>0.859</b>	
FKAN	0.76	0.74	0.82	0.78	0.57	0.58	0.68	0.78	0.60	0.63	0.64	0.68	0.80	0.77	0.74	0.72	14.2 (4.77)	0.704
Fast-KAN	0.71	0.81	0.84	0.75	0.57	0.53	0.66	0.71	0.63	0.62	0.73	0.70	<b>0.89</b>	0.85	0.70	0.70	13.8 (5.53)	0.713

## 4.5 Multi-class Classification

Table 4 compares TabKAN with other neural network models on two multi-class classification datasets. Because these tasks often suffer from sample imbalance, we used macro-F1 as the primary evaluation metric during training to ensure balanced performance across all classes [41]. All KAN variants consistently outperform the baselines, with JacobiKAN achieving the best overall results. Its use of Jacobi polynomials, which include additional parameters  $\alpha$  and  $\beta$  for shaping the polynomial basis, enables more flexible and precise kernel approximations, thereby capturing complex patterns more effectively.

**Table 4:** Comparison of different methods on SG and FO datasets.

Methods	SA		FO		Rank ↓
	ACC	F1	ACC	F1	
MLP	90.97	90.73	67.09	48.03	9.25 (0.5)
TabTrans	-	-	68.76	49.47	8.5 (0.707)
TabNet	96.09	94.96	65.09	52.52	7.25 (2.5)
<b>KAN</b>	96.32	96.33	85.11	84.80	4 (1.15)
<b>ChebyshevKAN</b>	<b>96.54</b>	<b>96.54</b>	82.67	82.38	4 (3.46)
<b>JacobiKAN</b>	<u>96.49</u>	<u>96.49</u>	<b>96.56</b>	<b>96.56</b>	<b>1.5 (0.577)</b>
<b>PadeRKN</b>	94.81	94.78	92.95	92.94	5.5 (2.89)
<b>Fourier KAN</b>	95.89	95.89	84.55	84.42	5.62 (0.479)
<b>fKAN</b>	95.89	95.93	<u>95.80</u>	<u>95.79</u>	<u>3.38 (1.70)</u>
<b>fast-KAN</b>	95.45	95.44	87.13	86.98	5.25 (1.5)

TabTrans does not have the capability to handle categorical input, so we could not run the SA dataset on it [41].

## 4.6 Interpretability

For interpretability purposes, there are two main approaches: model-specific methods and model-agnostic methods. Model-specific methods apply only to a particular model (e.g., in logistic regression, coefficients represent feature importance). In contrast, model-agnostic methods can be applied to any model, regardless of its type.

A defining strength of Kolmogorov-Arnold Networks (KAN) lies in their inherent interpretability, a critical advantage for domains requiring transparency in decision-making. Unlike traditional black-box models (e.g., deep neural networks or gradient-boosted trees), KANs explicitly parameterize univariate functions along network edges, enabling direct visualization of feature-wise contributions and functional mappings. This architectural design not only reduces reliance on post hoc interpretation methods but also aligns model behavior with domain-specific knowledge, fostering trust and facilitating model audits.

Figures 1, 2, and 3 illustrate the attribution of Feature 1 in the CA dataset towards the output, while Figures 4, 5, and 6 represent the attribution of Feature 2. Specifically, Figures 1 and 4 demonstrate the interpretability of the Fourier-based KAN, whereas Figures 2 and 5

highlight the interpretability of the Chebyshev-based KAN. The domain and codomain are normalized for these figures, which explains the difference in scale compared to the PDP figures. We employed Partial Dependence Plot (PDP) as a post-hoc analysis to assess the differences in feature interpretation.

In our framework, each feature’s learned univariate function provides non-parametric insights into its contribution to the final prediction. By visualizing these functions, we observe how individual features nonlinearly transform inputs, revealing monotonic trends, thresholds, or saturation effects that may correlate with domain expertise.

The model’s structure also facilitates analysis of feature interactions. While KANs primarily model univariate functions, multivariate interactions emerge implicitly through the additive composition of these functions in deeper layers. By analyzing co-variations in learned functions across related features, we infer latent dependencies and validate them against domain knowledge. For example, overlapping saturation points in two features’ functions may indicate synergistic effects.

Finally, the parametric nature of KANs ensures reproducibility in interpretation. Unlike post hoc methods (e.g., SHAP or LIME), which can vary with input perturbations, KANs provide consistent functional mappings tied directly to the model’s architecture.

## 4.7 Feature Importance and Dimensionality Reduction

We evaluate the feature importance and dimensionality reduction capabilities of the proposed TabKAN framework by analyzing the magnitude of coefficients derived from the Chebyshev and Fourier-based KAN equations. Specifically, we compute the absolute values of the coefficients from the Chebyshev equation in 1 and the Fourier equation in 2. Figure 7 depicts the ranked feature importance derived from the Chebyshev coefficients, while Figure 8 illustrates the corresponding rankings from the Fourier coefficients.

Based on these rankings, we conducted further experiments to assess the predictive performance of Fourier KAN and Chebyshev KAN models using subsets of features identified by their coefficients. Figures 9 and 10 illustrate the ROC-AUC performance across five datasets (CG, CA, DS, CB, BL) after varying levels of feature reduction. The results indicate that utilizing all available features does not necessarily yield the best predictive performance. In fact, for some datasets, models trained on reduced feature sets achieve comparable or even superior accuracy. This highlights TabKAN’s effectiveness in selecting compact, informative subsets of features, providing a valuable mechanism for supervised dimensionality reduction. Such an approach simplifies model interpretation and often enhances predictive robustness, further demonstrating the practical utility of the proposed TabKAN architectures.

Figure 11a reports the AUC values obtained using various subsets of top-ranked features identified by the proposed FourierKAN-based method, compared with those selected by SHAP analysis. The results demonstrate that model-specific feature importance consistently yields superior AUC performance when less significant features are removed. Similarly, experiments conducted with ChebyshevKAN using the CG and CB datasets (Figure 11b) reinforce the observation that the proposed approach outperforms SHAP-based feature selection in achieving stable and improved predictive accuracy. While there is some overlap in the selected features between the SHAP-based and model-specific methods, the proposed approach often provides more stable or higher predictive performance. This outcome highlights the advantage

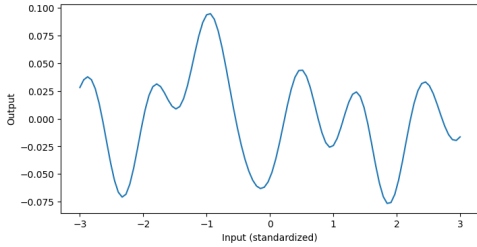


**Fig. 1:** Fourier KAN - Feature 1

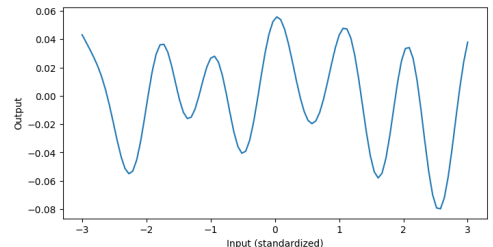


**Fig. 4:** Fourier KAN - Feature 2

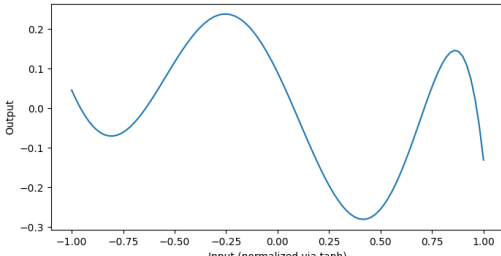


**Fig. 2:** ChebyshevKAN - Feature 1

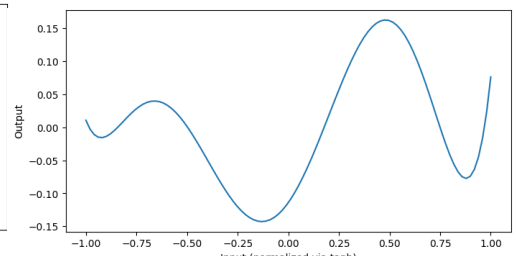


**Fig. 5:** ChebyshevKAN - Feature 2

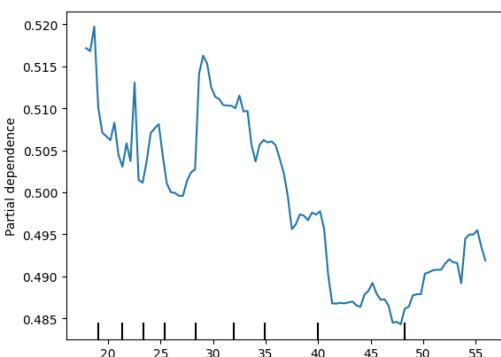


**Fig. 3:** Partial Dependence Plot - Feature 1

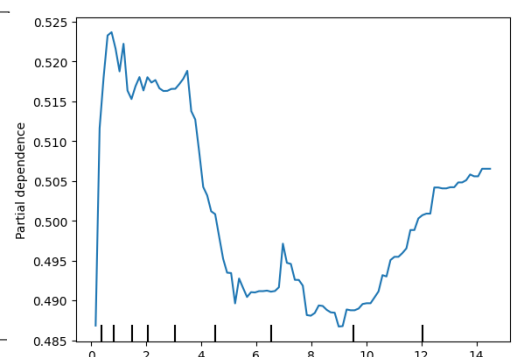


**Fig. 6:** Partial Dependence Plot - Feature 2

of using learned functional parameters as a built-in mechanism for feature selection, which is both efficient and closely aligned with the model’s internal representation.

## 5 Ablation Study

### 5.1 Fine-tuning:

In transfer learning scenarios, where a pre-trained model is adapted to a new task or domain, the **Group Relative Policy Optimization (GRPO)** [42] framework provides a robust mechanism for fine-tuning by strategically balancing task-specific adaptation with knowledge retention. Leveraging a policy gradient approach, GRPO optimizes model parameters  $\theta$  through advantage-weighted updates derived from reward signals ( $R \in \{0, 1\}$ ), where rewards

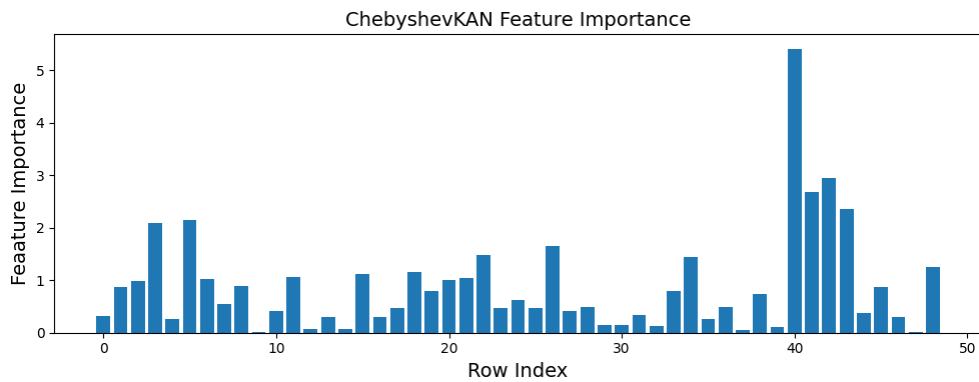


**Fig. 7:** Feature Importance

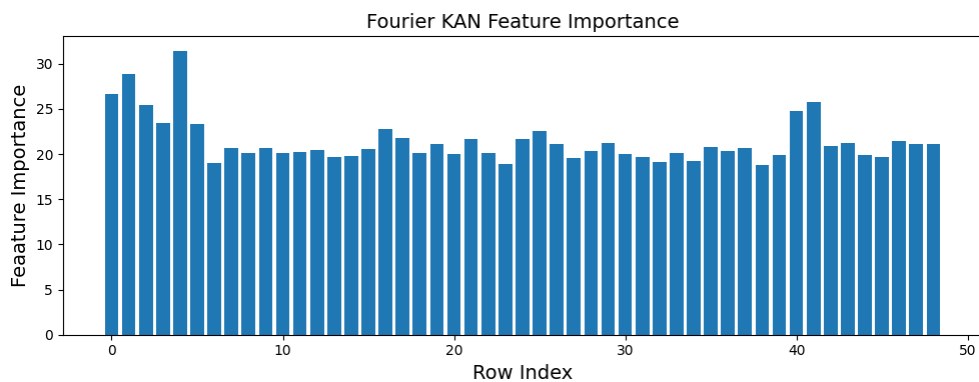


**Fig. 8:** Feature Importance

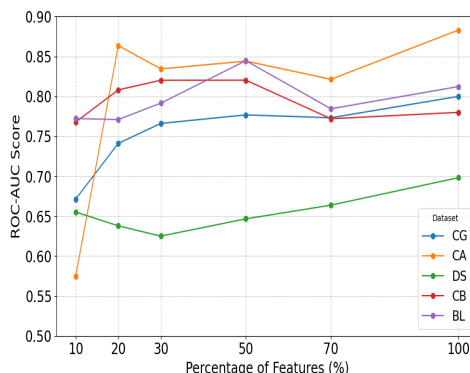


**Fig. 9:** AUC vs Percentage of Top Selected Features

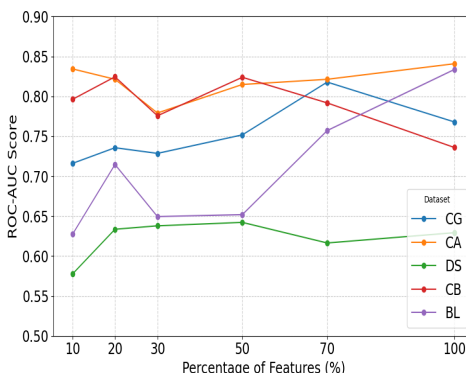
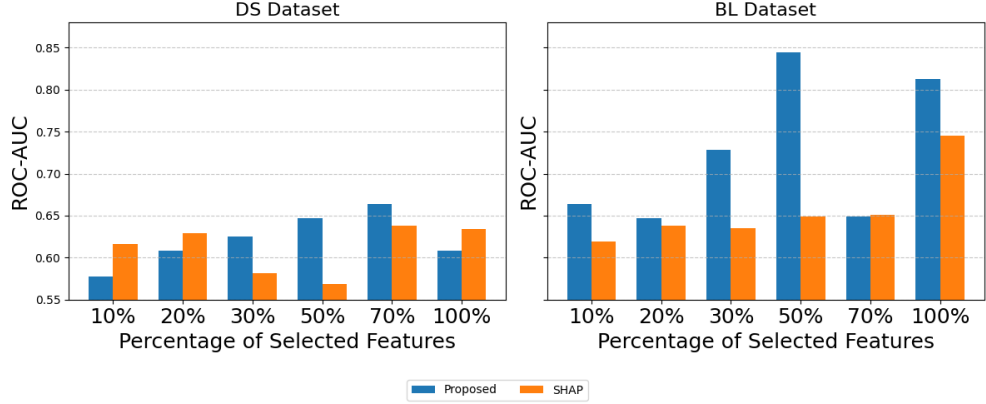
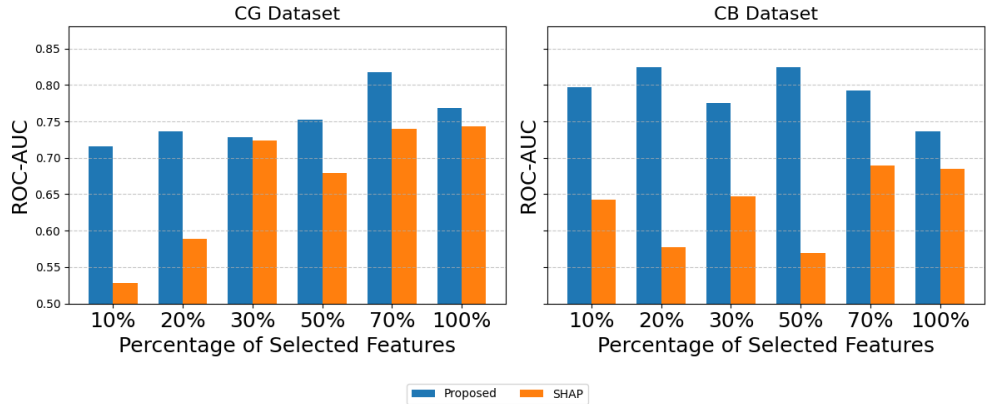


**Fig. 10:** AUC vs Percentage of Top Selected Features



(a) Comparison of Selective top important features in FourierKAN



(b) Comparison of Selective top important features in ChebyshevKAN

**Fig. 11:** Comparison of feature importance selection between the proposed method and SHAP across two datasets.

reflect alignment between sampled predictions ( $o \sim \pi_\theta$ ) and ground-truth labels. To mitigate catastrophic forgetting—a common challenge in transfer learning—the method incorporates a Kullback-Leibler (KL) divergence penalty  $\beta \cdot \mathbb{D}_{\text{KL}}(\pi_\theta \parallel \pi_{\text{ref}})$ , which constrains deviations from the reference policy  $\pi_{\text{ref}}$  (e.g., the original pre-trained model). By sampling  $G$  candidate predictions per input and computing normalized advantages  $\hat{A} = R - \mathbb{E}[R]$ , GRPO promotes exploration while maintaining stability, making it particularly suited for scenarios with limited target-domain data.

$$\begin{aligned}
\mathcal{J}_{\text{GRPO}}(\theta) &= \underbrace{\mathbb{E}_{\substack{q \sim \text{Batch} \\ o \sim \pi_\theta}} \left[ \frac{1}{G} \sum_{i=1}^G \log \pi_\theta(o_i | q) \cdot \hat{A}_i \right]}_{\text{Policy Gradient Loss}} + \underbrace{\beta \cdot \mathbb{E}_{q \sim \text{Batch}} [\mathbb{D}_{\text{KL}}(\pi_\theta(\cdot | q) \| \pi_{\text{ref}}(\cdot | q))]}_{\text{KL Divergence Penalty}} \\
\hat{A}_i &= R_i - \mathbb{E}[R_i] \quad (\text{Advantage}) \\
R_i &= \begin{cases} 1 & \text{if prediction } o_i = \text{label} \\ 0 & \text{otherwise} \end{cases} \\
\mathbb{D}_{\text{KL}}(\pi_\theta \| \pi_{\text{ref}}) &= \sum_{c \in \{0, 1\}} \pi_\theta(c | q) \log \frac{\pi_\theta(c | q)}{\pi_{\text{ref}}(c | q)}
\end{aligned}$$

$$\mathcal{J}_{\text{GRPO}}(\theta) = -\mathbb{E} [\log \pi_\theta(o | q) \cdot \hat{A}] + \beta \cdot \mathbb{E} [\mathbb{D}_{\text{KL}}(\pi_\theta \| \pi_{\text{ref}})]$$

## 5.2 Ablation on Enhanced Architecture

We conducted an ablation study to develop a KAN-based architecture. As KAN serves as an alternative to MLP, we applied it to the MLP-Mixer [43] block to construct a KAN-Mixer [44]. Specifically, we replaced all MLP blocks in [24] (Fig. 2) with alternative KAN layers, preserving the overall structure of the original architecture while leveraging the functional properties of KAN. The results show improvements on certain datasets compared to the KAN-based models in Table 5, with these improvements marked by an asterisk. This indicates that the KAN-Mixer outperforms both standard MLP-Mixer and basic KAN-based models on specific datasets, demonstrating its effectiveness in capturing complex patterns in tabular data. For reference, the results of the MLP-Mixer are taken from Table 2 in [24].

**Table 5:** Evaluation of Different Enhanced Models for Supervised Learning

Methods	CG	CA	DS	CB	BL	IO
<b>ChebyshevKAN-Mixer</b>	0.824*	0.863	0.706*	0.807	0.832	0.950
<b>JacobiKAN-Mixer</b>	0.817	0.876*	0.715*	0.767	0.843*	0.950
<b>Fourier KAN-Mixer</b>	0.850*	0.909*	0.715*	0.826*	0.707*	0.914

## 6 Conclusion

In this work, we introduced TabKAN, a novel Kolmogorov-Arnold Network-based architecture designed to advance tabular data analysis. By leveraging modular KAN-based models, we demonstrated their effectiveness in both supervised learning and transfer learning, where TabKAN significantly outperformed classical and Transformer-based models in knowledge

transfer tasks. Unlike conventional deep learning approaches that rely on post hoc interpretability methods, TabKAN introduces model-specific interpretability, allowing for direct visualization and analysis of feature interactions within the network. To further enhance the expressiveness and adaptability of KANs for tabular data learning, we utilized multiple specialized architectures, including ChebyshevKAN, JacobiKAN, PadeRKAN, FourierKAN, fKAN, and fast-KAN, each offering distinct advantages in function approximation and performance. Additionally, we introduced a new fine-tuning approach for transfer learning, improving the efficiency of knowledge transfer between domains. Furthermore, we enhanced the basic architecture by leveraging the advantages of KAN over MLP, leading to the development of more robust and scalable models for tabular data. Our extensive experiments across multiple benchmark datasets highlight the robustness, efficiency, and scalability of KAN-based architectures, bridging the gap between traditional machine learning and deep learning for structured data. Building on these advancements, future work will focus on further optimizing KAN architectures and extending their applicability to self-supervised learning and domain adaptation, enabling broader adoption of KANs in real-world applications.

## References

- [1] Liu, Z., Wang, Y., Vaidya, S., Ruehle, F., Halverson, J., Soljačić, M., Hou, T.Y., Tegmark, M.: Kan: Kolmogorov-arnold networks. arXiv preprint arXiv:2404.19756 (2024)
- [2] SS, S., AR, K., KP, A., et al.: Chebyshev polynomial-based kolmogorov-arnold networks: An efficient architecture for nonlinear function approximation. arXiv preprint arXiv:2405.07200 (2024)
- [3] Aghaei, A.A.: rkan: Rational kolmogorov-arnold networks. arXiv preprint arXiv:2406.14495 (2024)
- [4] Dong, Y., Li, G., Tao, Y., Jiang, X., Zhang, K., Li, J., Su, J., Zhang, J., Xu, J.: Fan: Fourier analysis networks. arXiv preprint arXiv:2410.02675 (2024)
- [5] Aghaei, A.A.: fkan: Fractional kolmogorov-arnold networks with trainable jacobi basis functions. arXiv preprint arXiv:2406.07456 (2024)
- [6] Li, Z.: Kolmogorov-arnold networks are radial basis function networks. arXiv preprint arXiv:2405.06721 (2024)
- [7] Maqbool, M.H., Fereidouni, M., Siddique, A., Foroosh, H.: Model-agnostic zero-shot intent detection via contrastive transfer learning. International Journal of Semantic Computing **18**(1) (2024)
- [8] Ye, A., Wang, Z.: Modern deep learning for tabular data: novel approaches to common modeling problems. Springer (2023)
- [9] Chen, T., Guestrin, C.: Xgboost: A scalable tree boosting system. Proceedings of ACM SIGKDD International Conference on Knowledge Discovery and Data Mining **22**, 785–794 (2016)
- [10] Zhang, Y., Tong, J., Wang, Z., Gao, F.: Customer transaction fraud detection using xgboost model. International Conference on Computer Engineering and Application (ICCEA), 554–558 (2020). IEEE
- [11] Klambauer, G., Unterthiner, T., Mayr, A., Hochreiter, S.: Self-normalizing neural networks. Advances in Neural Information Processing Systems **30**, 972–981 (2017)
- [12] Song, W., Shi, C., Xiao, Z., Duan, Z., Xu, Y., Zhang, M., Tang, J.: Autoint: Automatic feature interaction learning via self-attentive neural networks. ACM International Conference on Information and Knowledge Management, 1161–1170 (2019)
- [13] Wang, Z., Sun, J.: Transtab: Learning transferable tabular transformers across tables. Advances in Neural Information Processing Systems **35**, 2902–2915 (2022)
- [14] Huang, X., Khetan, A., Cvitkovic, M., Karnin, Z.: Tabtransformer: Tabular data modeling using contextual embeddings. arXiv preprint arXiv:2012.06678 (2020)

- [15] Somepalli, G., Goldblum, M., Schwarzschild, A., Bruss, C.B., Goldstein, T.: Saint: Improved neural networks for tabular data via row attention and contrastive pre-training. arXiv preprint arXiv:2106.01342 (2021)
- [16] Dorogush, A.V., Ershov, V., Gulin, A.: Catboost: gradient boosting with categorical features support. arXiv preprint arXiv:1810.11363 (2018)
- [17] Ke, G., Meng, Q., Finley, T., Wang, T., Chen, W., Ma, W., Ye, Q., Liu, T.-Y.: Lightgbm: A highly efficient gradient boosting decision tree. Advances in Neural Information Processing Systems **30** (2017)
- [18] Onishi, S., Oono, K., Hayashi, K.: Tabret: Pre-training transformer-based tabular models for unseen columns. arXiv preprint arXiv:2303.15747 (2023)
- [19] Zhu, B., Shi, X., Erickson, N., Li, M., Karypis, G., Shoaran, M.: Xtab: Cross-table pretraining for tabular transformers. arXiv preprint arXiv:2305.06090 (2023)
- [20] Zarlenga, M.E., Shams, Z., Nelson, M.E., Kim, B., Jamnik, M.: Tabcbm: Concept-based interpretable neural networks for tabular data. Transactions on Machine Learning Research (2023)
- [21] Hollmann, N., Müller, S., Purucker, L., Krishnakumar, A., Körfer, M., Hoo, S.B., Schirrmeister, R.T., Hutter, F.: Accurate predictions on small data with a tabular foundation model. Nature **637**(8045), 319–326 (2025)
- [22] Yan, R., Islam, M.T., Xing, L.: Interpretable discovery of patterns in tabular data via spatially semantic topographic maps. Nature Biomedical Engineering, 1–12 (2024)
- [23] Li, J., Qian, R., Tan, Y., Li, Z., Chen, L., Liu, S., Wu, J., Chai, H.: Tabsal: Synthesizing tabular data with small agent assisted language models. Knowledge-Based Systems **304**, 112438 (2024)
- [24] Eslamian, A., Cheng, Q.: Tabmixer: advancing tabular data analysis with an enhanced mlp-mixer approach. Pattern Analysis and Applications **28**(2), 1–17 (2025)
- [25] Liu, Z., Wang, Y., Vaidya, S., Ruehle, F., Halverson, J., Soljačić, M., Hou, T.Y., Tegmark, M.: Kan: Kolmogorov-arnold networks. arXiv preprint arXiv:2404.19756 (2024)
- [26] Ba, J.L., Kiros, J.R., Hinton, G.E.: Layer normalization. arXiv preprint arXiv:1607.06450 (2016)
- [27] Akiba, T., Sano, S., Yanase, T., Ohta, T., Koyama, M.: Optuna: A next-generation hyperparameter optimization framework. In: Proceedings of the 25th ACM SIGKDD International Conference on Knowledge Discovery & Data Mining, pp. 2623–2631 (2019)
- [28] Xu, J., Chen, Z., Li, J., Yang, S., Wang, W., Hu, X., Ngai, E.C.-H.: Fourierkan-gcf: Fourier kolmogorov-arnold network—an effective and efficient feature transformation for

graph collaborative filtering. arXiv preprint arXiv:2406.01034 (2024)

[29] Aghaei, A.A.: fkan: Fractional kolmogorov–arnold networks with trainable jacobi basis functions. *Neurocomputing* **623**, 129414 (2025)

[30] Aghaei, A.A.: rkan: Rational kolmogorov-arnold networks. arXiv preprint arXiv:2406.14495 (2024)

[31] Arik, S.Ö., Pfister, T.: Tabnet: Attentive interpretable tabular learning. In: Proceedings of the AAAI Conference on Artificial Intelligence, vol. 35, pp. 6679–6687 (2021)

[32] Wang, R., Fu, B., Fu, G., Wang, M.: Deep & cross network for ad click predictions. *Proceedings of the ADKDD’17* (2017) <https://doi.org/10.1145/3124749.3124754>

[33] Gorishniy, Y., Rubachev, I., Khrulkov, V., Babenko, A.: Revisiting deep learning models for tabular data. *Advances in Neural Information Processing Systems* **34**, 18932–18943 (2021)

[34] Yoon, J., Zhang, Y., Jordon, J., Schaar, M.: Vime: Extending the success of self-and semi-supervised learning to tabular domain. *Advances in Neural Information Processing Systems* **33**, 11033–11043 (2020)

[35] Bahri, D., Jiang, H., Tay, Y., Metzler, D.: Scarf: Self-supervised contrastive learning using random feature corruption. arXiv preprint arXiv:2106.15147 (2021)

[36] Bozorgasl, Z., Chen, H.: Wav-kan: Wavelet kolmogorov-arnold networks. arXiv preprint arXiv:2405.12832 (2024)

[37] Ta, H.-T., Thai, D.-Q., Rahman, A.B.S., Sidorov, G., Gelbukh, A.: Fc-kan: Function combinations in kolmogorov-arnold networks. arXiv preprint arXiv:2409.01763 (2024)

[38] Deldadehasl, M., Karahroodi, H.H., Nekah, P.H.: Customer clustering and marketing optimization in hospitality: A hybrid data mining and decision-making approach from an emerging economy (2025)

[39] Su, A., Wang, A., Ye, C., Zhou, C., Zhang, G., Chen, G., Zhu, G., Wang, H., Xu, H., Chen, H., et al.: Tablegpt2: A large multimodal model with tabular data integration. arXiv preprint arXiv:2411.02059 (2024)

[40] Huang, W.: Multimodal contrastive learning and tabular attention for automated alzheimer’s disease prediction. In: Proceedings of the IEEE/CVF International Conference on Computer Vision, pp. 2473–2482 (2023)

[41] Gao, W., Gong, Z., Deng, Z., Rong, F., Chen, C., Ma, L.: Tabkanet: Tabular data modeling with kolmogorov-arnold network and transformer. arXiv preprint arXiv:2409.08806 (2024)

[42] Shao, Z., Wang, P., Zhu, Q., Xu, R., Song, J., Bi, X., Zhang, H., Zhang, M., Li, Y., Wu,

Y., et al.: Deepseekmath: Pushing the limits of mathematical reasoning in open language models. arXiv preprint arXiv:2402.03300 (2024)

- [43] Tolstikhin, I.O., Houlsby, N., Kolesnikov, A., Beyer, L., Zhai, X., Unterthiner, T., Yung, J., Steiner, A., Keysers, D., Uszkoreit, J., *et al.*: Mlp-mixer: An all-mlp architecture for vision. *Advances in neural information processing systems* **34**, 24261–24272 (2021)
- [44] Ibrahum, A.D.M., Shang, Z., Hong, J.-E.: How resilient are kolmogorov–arnold networks in classification tasks? a robustness investigation. *Applied Sciences* **14**(22), 10173 (2024)

## Appendix A Hyperparameter Sensitivity

This appendix provides a detailed analysis of the hyperparameter sensitivity across seven neural network models (fastKAN, rKAN, fKAN, ChebKAN, KAN, FourierKAN) evaluated on eight datasets (IO, IC, DS, CG, CB, CA, BL, AD). The analysis focuses on four key architectural metrics: Layers, Neurons, Order, and Grid, as summarized in Tables ??.

The architectural complexity of the models varies significantly, with distinct patterns emerging in terms of depth, width, and approximation strategies. The rKAN and fKAN models consistently employ the highest number of layers, with rKAN reaching up to 7.7 layers in the BL dataset and fKAN averaging 7.5 layers in the IC and CA datasets. This suggests a reliance on depth to capture complex patterns. In contrast, fastKAN and ChebKAN use fewer layers, typically ranging from 1.5 to 3.5 on average, favoring simpler architectures. The variability in the number of layers is particularly high for rKAN and ChebKAN, as indicated by their large standard deviations (e.g., ChebKAN: std=2.6 in DS), reflecting dataset-specific adjustments in depth.

In terms of width, ChebKAN consistently uses the most neurons, with means ranging from 114 to 134 across datasets, followed by fastKAN, which averages between 105 and 149 neurons. This indicates a preference for wide, high-capacity layers. On the other hand, KAN and FourierKAN are the most compact, with KAN averaging 11.7 to 41.1 neurons and FourierKAN averaging 33.1 to 46.9 neurons. The stability of neuron counts also varies across models. KAN exhibits low variability (std=3.8–8.4), suggesting consistent architectural choices, while ChebKAN and fastKAN show high variability (e.g., ChebKAN: std=57.9 in BL), indicating dataset-specific tuning.

The order of basis functions, which reflects the complexity of the approximation, also varies across models. ChebKAN and fKAN use the highest-order basis functions, with ChebKAN averaging 4.2 to 5.4 and fKAN averaging 3.0 to 4.1. This likely enables precise approximations but may increase computational cost. In contrast, KAN uses the lowest order, averaging 1.1 to 2.9, favoring simpler models. Notably, fastKAN and FourierKAN do not use order parameters, implying fixed or non-polynomial basis functions.

Grid-based approximations are employed by KAN and FourierKAN, with FourierKAN utilizing the largest grids, averaging 10.2 in the BL dataset. This suggests the use of grid-based methods, such as Fourier transforms or splines, to achieve adaptive resolution. The variability in grid sizes is significant, particularly for FourierKAN (std=2.6 in BL), indicating adjustments based on dataset complexity.

Dataset-specific trends further highlight the adaptability of these models. For example, in the IO dataset, ChebKAN uses the widest layers (mean=121 neurons), while KAN is the most efficient (mean=41.1 neurons). In the IC dataset, KAN has the smallest architecture (mean=13.7 neurons), contrasting with fastKAN (mean=149.3 neurons). The AD dataset showcases ChebKAN using the highest order (mean=5.4), while fastKAN has the lowest neuron count (mean=46.4) but higher depth (mean=3.5 layers). In the BL dataset, rKAN and fKAN are the deepest (mean=7.7 and 6.4 layers, respectively), while FourierKAN uses the largest grid (mean=10.2).

The trade-offs between depth, width, and approximation strategies are evident. Models like rKAN and fKAN prioritize depth, while ChebKAN and fastKAN emphasize width. KAN strikes a balance, maintaining compact architectures. The choice of approximation strategy also varies, with ChebKAN and fKAN relying on high-order polynomials for accuracy, and

KAN and FourierKAN using grid-based methods. Low-variability models, such as KAN, offer consistency, while high-variability models, such as ChebKAN, adapt to dataset complexity.

For practitioners, these insights provide guidance on model selection. ChebKAN or fastKAN are suitable for high-dimensional data due to their wide layers and high capacity. KAN and FourierKAN are ideal for efficiency, given their compact architectures and grid-based approximations. For tasks requiring the capture of complex patterns, rKAN and fKAN leverage depth and high-order approximations effectively.

Model	Layers		Neurons		Order		Grid	
	Mean	Std.	Mean	Std.	Mean	Std.	Mean	Std.
fastKAN	1.3	0.5	144.5	39.2	-	-	-	-
JacobiRKAN	1.5	0.8	77.0	13.0	2.2	0.4	-	-
PadéRKAN	2.8	1.4	124.7	30.1	(5.0, 2.3)	(0.6, 0)	-	-
fKAN	4.9	1.1	71.1	11.1	3.9	0.6	-	-
ChebKAN	2.1	0.3	123.2	25.1	4.9	0.3	-	-
KAN	1.0	0.0	40.0	0.0	1.0	0.0	7.0	0.0
FourierKAN	2.6	0.6	37.2	6.3	-	-	1.9	0.6

**Table A1:** IO Dataset

Model	Layers		Neurons		Order		Grid	
	Mean	Std.	Mean	Std.	Mean	Std.	Mean	Std.
fastKAN	2.4	0.7	156.2	20.5	-	-	-	-
JacobiRKAN	1.9	1.5	19.0	10.0	3.7	0.6	-	-
PadéRKAN	4.0	1.2	98.0	39.6	(4.5, 2.9)	(0.5, 1)	-	-
fKAN	7.6	1.8	43.3	7.9	3.9	0.4	-	-
ChebKAN	1.0	0.0	141.4	36.4	5.1	0.6	-	-
KAN	2.0	0.0	10.0	0.0	1.0	0.0	5.0	0.0
FourierKAN	1.0	0.2	52.9	10.1	-	-	4.5	3.0

**Table A2:** IC Dataset

## Appendix B Consistency Across 100 Seed Values

Our experiments reveal that the choice of seed plays a crucial role in influencing the results. This effect is particularly evident during the data partitioning process for training and testing. To capture this variability, we illustrate the interquartile range, offering a broader perspective on the fluctuations in our findings, as depicted in Fig. B1. This analysis highlights both the

Model	Layers		Neurons		Order		Grid	
	Mean	Std.	Mean	Std.	Mean	Std.	Mean	Std.
fastKAN	1.4	0.7	105.8	35.9	-	-	-	-
JacobiRKAN	4.6	2.3	59.1	11.1	3.2	0.7	-	-
PadéRKAN	10.7	7.0	92.5	29.3	(3.9, 3.7)	(0.3, 1)	-	-
fKAN	7.4	1.8	58.6	7.6	4.0	0.4	-	-
ChebKAN	2.1	0.6	125.1	40.2	4.6	0.7	-	-
KAN	3.6	0.5	20.4	2.8	3.0	0.0	3.0	0.0
FourierKAN	2.1	0.4	39.4	8.1	-	-	6.6	1.5

**Table A3:** DS Dataset

Model	Layers		Neurons		Order		Grid	
	Mean	Std.	Mean	Std.	Mean	Std.	Mean	Std.
fastKAN	1.7	0.8	116.0	27.6	-	-	-	-
JacobiRKAN	1.4	0.8	86.9	13.6	2.4	0.6	-	-
PadéRKAN	3.0	1.3	126.7	27.6	(4.8, 3.2)	(0.7, 0)	-	-
fKAN	3.3	1.9	70.7	12.9	2.9	0.5	-	-
ChebKAN	2.6	0.5	116.0	20.4	4.3	0.7	-	-
KAN	3.0	0.0	26.7	0.0	3.0	0.0	5.0	0.0
FourierKAN	2.4	0.7	38.4	9.3	-	-	2.1	1.0

**Table A4:** CG Dataset

stability of our model and the inevitable variations in performance stemming from different data splits.

Model	Layers		Neurons		Order		Grid	
	Mean	Std.	Mean	Std.	Mean	Std.	Mean	Std.
fastKAN	1.3	0.6	113.7	34.7	-	-	-	-
JacobiRKAN	2.8	2.1	70.2	16.3	3.0	0.3	-	-
PadéRKAN	15.2	5.7	105.7	8.9	(4.0, 4.3)	(0.2, 0)	-	-
fKAN	3.4	1.0	44.4	11.0	3.2	0.6	-	-
ChebKAN	2.5	0.5	122.1	30.9	4.4	0.5	-	-
KAN	3.0	0.0	10.0	0.0	1.0	0.0	5.0	0.0
FourierKAN	2.3	0.5	34.7	11.9	-	-	2.6	0.8

**Table A5:** CB Dataset

Model	Layers		Neurons		Order		Grid	
	Mean	Std.	Mean	Std.	Mean	Std.	Mean	Std.
fastKAN	2.8	0.7	126.9	23.6	-	-	-	-
JacobiRKAN	1.2	0.8	64.3	23.5	2.2	0.6	-	-
PadéRKAN	3.4	2.0	99.9	24.0	(5.0, 3.6)	(0.6, 1)	-	-
fKAN	7.4	1.5	56.9	8.3	3.9	0.4	-	-
ChebKAN	2.0	0.8	118.4	31.0	2.3	0.5	-	-
KAN	6.7	0.5	26.0	1.6	1.0	0.1	1.0	0.2
FourierKAN	2.3	0.5	32.4	7.1	-	-	4.8	1.3

**Table A6:** CA Dataset

Model	Layers		Neurons		Order		Grid	
	Mean	Std.	Mean	Std.	Mean	Std.	Mean	Std.
fastKAN	2.5	0.7	113.8	23.5	-	-	-	-
JacobiRKAN	8.0	1.5	70.3	7.3	3.5	0.4	-	-
PadéRKAN	2.3	1.6	137.3	32.2	(4.4, 2.4)	(0.7, 1)	-	-
fKAN	6.4	0.9	66.2	8.3	3.6	0.4	-	-
ChebKAN	1.1	0.3	130.3	64.5	4.0	1.4	-	-
KAN	2.0	0.2	35.4	3.3	1.0	0.1	6.1	1.1
FourierKAN	1.0	0.1	35.1	9.7	-	-	11.0	2.3

**Table A7:** BL Dataset

Model	Layers		Neurons		Order		Grid	
	Mean	Std.	Mean	Std.	Mean	Std.	Mean	Std.
fastKAN	3.6	1.8	35.8	22.1	-	-	-	-
JacobiRKAN	3.5	1.2	24.2	10.9	2.9	0.4	-	-
PadéRKAN	2.7	1.4	121.1	26.9	(3.8, 4.4)	(0.8, 1)	-	-
fKAN	5.4	1.8	33.0	7.3	3.3	0.8	-	-
ChebKAN	1.0	0.2	44.9	26.5	5.7	0.8	-	-
KAN	4.3	0.7	24.3	1.8	2.0	0.0	3.0	0.0
FourierKAN	1.0	0.2	44.9	8.1	-	-	8.8	2.7

**Table A8:** AD Dataset

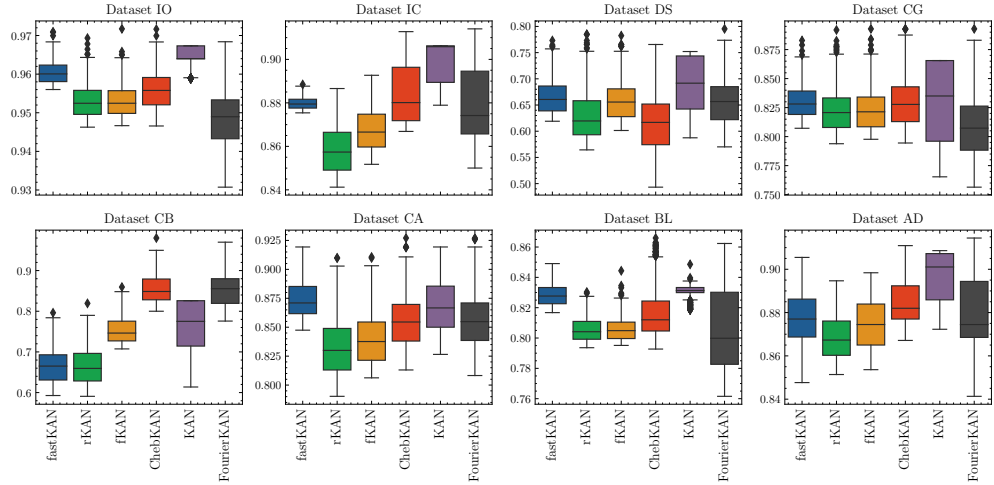


**Fig. B1:** The interquartile range across 100 runs with varying seed values highlights the influence of random seed selection on experimental outcomes. The plot depicts the variation in the distribution of raw and synthesized data across different training and test set splits.